JOURNAL OF SCIENTIFIC RESEARCH IN ALLIED SCIENCES
ISSN NO. 2455-5800
Contents available at www.jusres.com

Analysis and Optimization of Elastic Behaviour of ABS Plastic Using Fuzzy TOPSIS

Shubham Kumar Sinha[1], Jaykishan Gupta[2], Shailesh Dewangan[3]
[1]*M. Tech. Scholar, Chouksey Engineering College, Bilaspur C.G.*
[2,3]*Assistant professor, Chouksey Engineering College, Bilaspur C.G.*

ARTICLE INFO **ABSTRACT** **ORIGINAL RESEARCH ARTICLE**

Article History
Received: Dec. 2023
Accepted: Jan. 2024
Keywords:
Acrylonitrile Butadiene Styrene (ABS); 3D Printing; Fused Deposition Modeling; Fuzzy TOPSIS; Rapid Prototyping

Corresponding Author
***S. K. Sinha**

3D printing has revolutionized rapid prototyping and small-scale production, with Fused Deposition Modeling (FDM) emerging as a prominent method among various techniques. FDM utilizes thermoplastic filaments like Acrylonitrile Butadiene Styrene (ABS) to build objects layer by layer from digital designs. The proposed methodology is applied to a case study involving the design and manufacturing of an ABS plastic component with specific elastic behavior requirements. Through systematic experimentation and analysis, the optimal set of material parameters and process parameters are identified, leading to improved elastic performance while considering the inherent uncertainties in the system. Comparative analyses demonstrate the effectiveness and superiority of the fuzzy TOPSIS-based approach over traditional optimization techniques. This study delves into the elastic behaviors of ABS plastic and its optimization for enhanced performance. By employing techniques such as Fuzzy TOPSIS, the research aims to improve ABS plastic's elastic modulus, tensile strength, and hardness other pertinent properties. Initial experimentation involves evaluating ABS plastic's elasticity under diverse conditions, considering factors like temperature, pressure, and material composition. Subsequent analysis identifies key parameters influencing ABS plastic's elasticity, paving the way for optimization using Fuzzy TOPSIS.

1. INTRODUCTION

3D printing is a manufacturing process where objects are created layer by layer from digital designs. It is also known as Additive Manufacturing. It allows for rapid prototyping, customization, and production of complex geometries. Unlike traditional subtractive manufacturing methods, which involve removing material from a larger block, 3D printing adds material incrementally[1]. Creating a digital model using computer-aided design (CAD) software is the initial process. Various 3D printing technologies exist, each with its own principles and materials. A notable method is Fused Deposition Modeling (FDM), where a thermoplastic filament is heated until it becomes molten and then extruded through a nozzle[2].

ABS (Acrylonitrile Butadiene Styrene) plastic is widely used in manufacturing due to its excellent mechanical properties, including toughness, impact resistance, and elastic behavior. The performance of ABS components is influenced by several factor like material parameters and process parameter. For instance, Hazim et. al [3] emphasized the importance of precise temperature control during injection molding to achieve desired

mechanical properties. Traditional optimization techniques for selecting material and process parameters frequently include methods like Design of Experiments (DOE), Response Surface Methodology (RSM), and Taguchi methods[4]. These approaches have been successfully employed to determine significant factors and their optimal levels for enhancing product quality and performance. Nevertheless, they can sometimes struggle to effectively address the uncertainties inherent in manufacturing processes [5].

Recent studies have demonstrated the superiority of fuzzy TOPSIS in optimizing complex manufacturing processes. Applied fuzzy TOPSIS to optimize the injection molding parameters of ABS plastic parts, leading to significant improvements in product quality and performance[6]. Comparative analyses in these studies have shown that fuzzy TOPSIS-based approaches can outperform traditional optimization techniques by providing more accurate and reliable results under uncertain conditions.

Acrylonitrile Butadiene Styrene (ABS) plastic is widely utilized in various industries due to its excellent balance of properties such as impact resistance, toughness, and ease of machining. This study investigates the elastic behavior of ABS plastic and explores optimization techniques using Fuzzy TOPSIS method to enhance its performance, focusing on properties like tensile strength, and hardness[7].

2. MATERIAL AND METHOD

2.1 ABS (Acrylonitrile Butadiene Styrene) material

ABS (Acrylonitrile Butadiene Styrene) plastic is a thermoplastic polymer renowned for its versatility, durability, and ease of processing. The material consists of three monomers: acrylonitrile, butadiene, and styrene. Acrylonitrile, synthesized from propylene and ammonia, contributes to the plastic's strength and rigidity. Butadiene, a petroleum hydrocarbon derived from butane, imparts toughness and impact resistance. Styrene, sourced from benzene and ethylene, enhances the material's processability and rigidity[3].

The Chemical Formula of ABS plastic: $(C_8H_8)_x.(C_4H_6)_y.(C_3H_3N)_z$

The characteristics of ABS plastic material are detailed in Table 1. Applications of ABS plastic span various industries, including automotive, electronics, and construction, where it is used for pipes, fittings, and architectural moldings. In 3D printing, ABS is commonly employed in filament-based printing using FDM technology. Additionally, ABS is suitable for post-processing techniques such as machining, painting, and adhesive bonding, making it a highly versatile material for manufacturers[8].

Table:1 Properties of ABS

Mechanical Properties	Density (g/cm^3)	Tensile Strength (MPa)	Elastic Limit (MPa)	Young's Modulus (GPa)	Poisson Ratio	Elongation at break in (%)	Stress at break (MPa)
Values	1.02-1.21	43.8	38.45	2.0-2.6	0.3	7.2	29.58

2.2 Rapid Prototyping Process

Additive manufacturing, commonly known as 3D printing, has emerged as a transformative technology that converts digital designs into tangible objects layer by layer. Unlike traditional manufacturing methods that involve cutting away material from a solid block, 3D printing builds up objects from scratch, offering unprecedented flexibility and versatility. Central to the 3D printing process is the creation of a digital model using computer-aided design (CAD) software[9]. This digital blueprint serves as the foundation for the physical object. Once the design is complete, the 3D printer interprets the model and proceeds to fabricate the object, meticulously laying down material layer by layer.

The nozzle moves across the build platform, depositing the melted material layer

by layer according to the specifications of the digital model. As each layer cools and solidifies, it fuses with the previous ones, gradually forming the complete object[10]. Rapid Prototyping (RP), a subset of 3D printing, has gained popularity for its ability to manufacture complex parts or assemblies in significantly less time than traditional methods that process is presented in Fig.1. RP processes fabricate physical parts directly from CAD data without human intervention, adding material layer by layer in the x-y plane, with material addition occurring in the z-direction[11]. This process is also known as Additive Manufacturing (AM), Solid Freeform Fabrication (SFF), Layered Manufacturing (LM), or Automated Fabrication (AF).

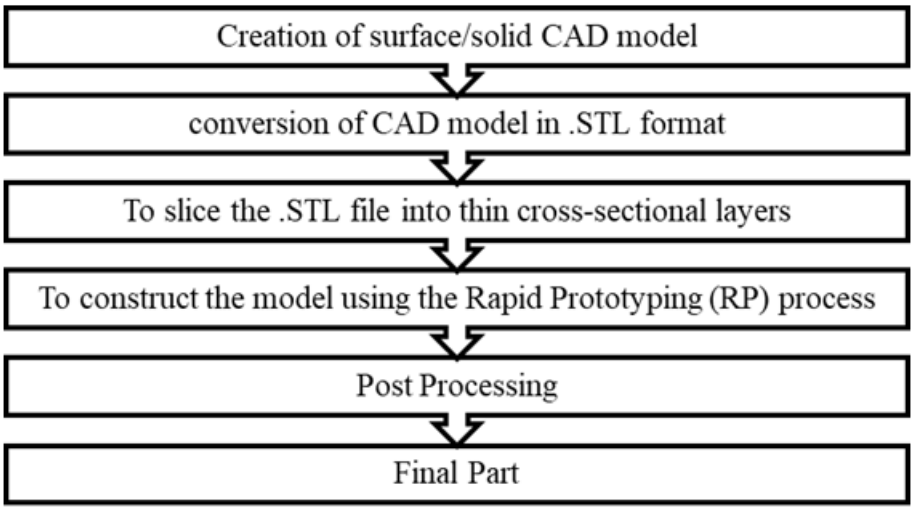

Fig 1: Rapid Prototyping Process

3. EXPERIMENTAL ANALYSIS

3.1 Section of workpiece

ASTM D638 Type-IV refers to a specific standard within the ASTM D638 series that addresses the tensile properties of plastics. This standard is a widely recognized test method for determining the tensile properties of both unreinforced and reinforced plastics using standard dumbbell-shaped test specimens[12]. Thin sheet materials typically have a thickness less than 1.0 mm (0.04 in) and may include materials such as films, laminates, and thin sheet products is shown in Fig. 2.

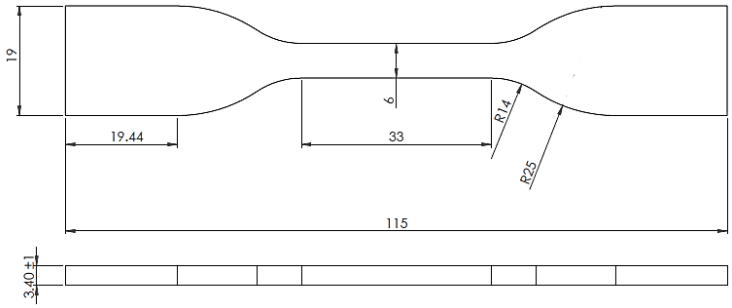

Fig 2: ASTM D638 Type-IV[13]

Type-IV specifies the testing procedure for testing thin sheet materials. When performing tensile tests in accordance with ASTM D638 Type-IV, it is essential to adhere to the specific requirements and procedures detailed in the standard to maintain consistency and accuracy

in the results. This encompasses the preparation of specimens, the testing conditions (including temperature and humidity), and the methods used for data analysis. The Standard Tessellation Language (STL) is a commonly used file format for 3D models. Table 2 presents the details of the 3D model file format[12].

Table 2 Parameters of 3D-Printer

Sample	Resolution	Layer Height (mm)	First Layer Height (mm)	Travel Speed (mm/s)	Print Speed (mm/s)
1	Low	0.30	0.30	100	80
2	Standard	0.18	0.27	80	60
3	High	0.14	0.21	70	50
4	Hyper	0.08	0.20	70	50

Normals are vectors that are perpendicular to the surface of a triangle in a 3D model. In an STL file, each triangular face has an associated normal vector. For successful 3D printing, ensure that your STL file is manifold (watertight) and that all normals are correctly oriented outwards. Use appropriate software tools to check and repair your model before slicing. By following these steps, you can create complex, printable 3D models without issues[5].

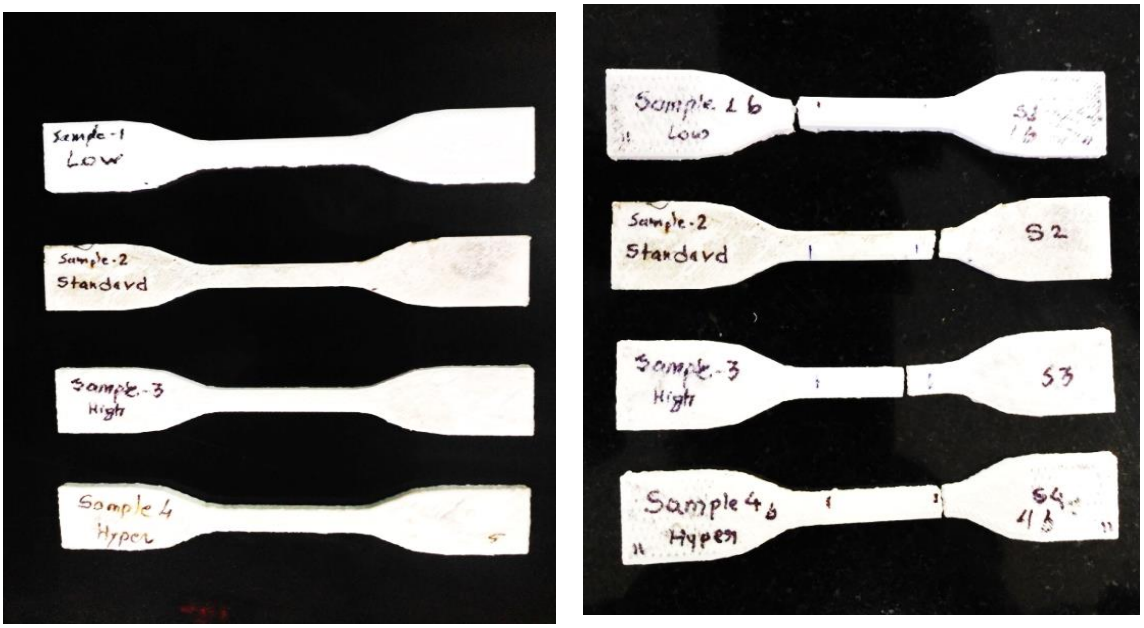

Fig 3: 3D printed ABS specimens' image before and after Tensile Test

3.2 Tensile Test

The engineering tension test stands as a pivotal method in comprehending the strength and characteristics of materials, serving both as a design tool and an acceptance test for material specifications [13]. Throughout this test, a specimen undergoes a progressively increasing uniaxial tensile force while its elongation is meticulously monitored. These observations are then utilized to construct an engineering stress-strain curve [15]. By precisely measuring the applied load and the

subsequent elongation, engineers can chart the stress-strain relationship of the material. This curve furnishes invaluable insights into the material's behavior under tensile stress, and the load-extension graphs of various workpiece specimens are depicted in Fig. 4. It is obtained by dividing the load by the original area of the cross section of the specimen.

$$\sigma = \frac{P}{A}$$

Where σ = average longitudinal stress, P = load, A = original area

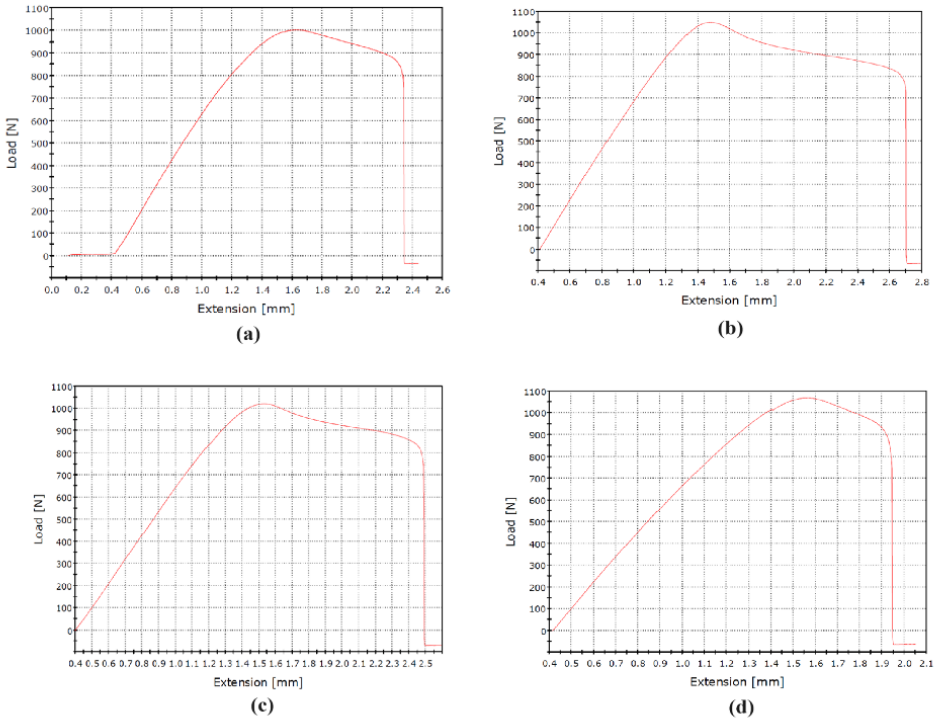

Fig.4 Load extension graph for different workpiece specimen

3.3 Hardness Test

Hardness typically refers to a material's resistance to deformation, particularly in metals where it indicates their ability to resist permanent or plastic deformation. In the field of material testing mechanics, hardness is primarily understood as the material's resistance to indentation. For design engineers, however, hardness is a convenient and easily measurable parameter that reveals important information about a metal's strength and the efficacy of its heat treatment[14]. Hardness can be measured in three main ways: scratch hardness, indentation hardness, and rebound (or dynamic) hardness. Of these methods, indentation hardness is particularly significant in engineering applications, as it provides essential data on a material's mechanical properties and its appropriateness for various uses[15].

The Vickers hardness test employs a diamond pyramid with a square base as its indenter, featuring opposing faces that create a 136-degree included angle. This specific angle is chosen to closely match the desired indentation-to-ball diameter ratio found in the Brinell hardness test. Due to the distinctive shape of the indenter, the test is often referred to as the diamond-pyramid hardness test[16]. The Vickers hardness number (VHN or VPH) is calculated by dividing the applied load by the surface area of the indentation. VHN is also known as the diamond-pyramid hardness number (DPH), is calculated by dividing the applied load by the surface area of the indentation. The surface area is determined

through microscopic measurements of the lengths of the diagonals of the indentation. As illustrated in Fig. 5, the impression is observed manually, and the measurements are recorded. The DPH can be determined using the equation 1.

$$DPH = \frac{2P\sin(\theta/2)}{L^2} = \frac{1.854P}{L^2} \quad (1)$$

Here, P is the applied load (kg),
L is the average length of diagonals (mm),
θ is the angle between opposite faces of diamond which is equal to 136°

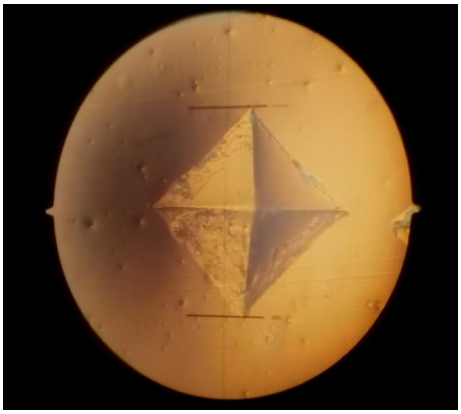

Fig 5: Micro Hardness Tester: SHIMADZU HMV Series

The experimental value of the Hardness and tensile test is tabulated in Table 3. According to this table L1 and L2 is the diagonal length of impression with horizonal and vertical simultaneously. And Hv is hardness value and Tensile stress unit is MPa.

Table 3. Observation of Hardness Test and Tensile test

Run NO.	L1 (µm)	L2 (µm)	Average Length L(µm)	Hv	Tensile Stress (MPa)
1	230.56	233.32	231.94	17.2	35.30
2	214.84	208.82	211.83	20.6	40.91
3	221.22	213.70	217.46	19.6	36.59
4	210.43	200.69	205.56	21.9	39.26
5	211.56	198.40	204.98	22.0	40.23
6	209.41	215.04	212.22	20.5	41.95
7	217.39	222.96	220.17	19.1	30.25
8	215.44	217.84	216.64	19.7	39.86
9	218.46	217.77	218.11	19.4	35.16
10	210.06	220.71	215.38	19.9	40.12
11	216.11	216.11	216.13	19.8	41.59
12	216.12	214.35	215.23	20.0	40.89

3.4 Surface Morphology Analysis of ABC plastic

Hardness Test is done on the Micro Hardness Tester: SHIMADZU HMV Series. For this test, a small sample is cut off the specimen and then mounted in the mount by cold setting process[8]. For hardening the liquid, acrylic powder is spread firmly over the hardener liquid layer by layer. After 4-5 minutes when the mixture is hardened, work-piece with the cold hardened moulds is taken out of the mount, that process is shown in Fig. 6.

Fig 6: Cold Setting using Hardener in the Moulds

Then surface is first grinded on the Belt Grinder and then polished over 5 different polishing papers (made of Silicon Carbide) of different grit sizes, ranging from 220 to 1200[17]. After that the work-piece is very finely polished in the Disc Grinder Polisher Machine, in which Alumina Powder of Grade-1 of size 1 microns is used[18]. Then, the surface of the work-piece becomes scratch free and no craters are present on its surface. An image of polished surface is shown in Fig. 7.

Fig 7: Workpiece Grinded in the Belt Grinder & Polishing with Silicon Carbide Paper

The surface of the workpiece under the Zeiss Axio microscope image is shown in Fig. 8. This image presents the surface morphology of ABC plastic material, and given information shape of a cell, and grin size.

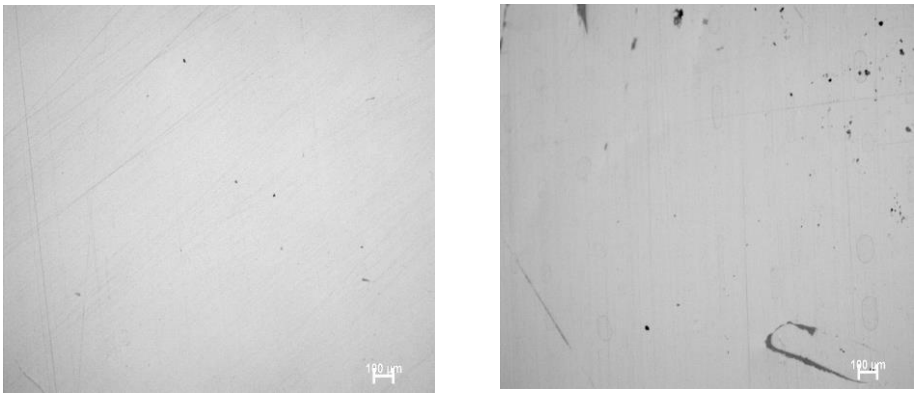

Fig. 8 Surface of the workpiece viewed through the Zeiss Axio Microscope

4. OPTIMIZATION TECHNIQUES

4.1 The Fuzzy TOPSIS

The Fuzzy TOPSIS method extends the traditional TOPSIS technique for multi-criteria decision-making. TOPSIS stands for Technique for Order Preference by Similarity to Ideal Solution. In the standard TOPSIS approach, criteria weights and decision matrix entries are treated as precise and deterministic[6]. However, Fuzzy TOPSIS accommodates imprecise information by utilizing fuzzy sets. This fuzzy logic-based approach has gained popularity in optimizing various manufacturing processes, such as enhancing tensile strength and hardness. The Fuzzy TOPSIS method ranks options based on their proximity to an ideal solution[19], effectively managing uncertainties and imprecisions in decision-making by utilizing fuzzy sets. Thus, Fuzzy TOPSIS serves as a robust decision-making tool that evaluates and prioritizes alternatives in the presence of uncertainty.

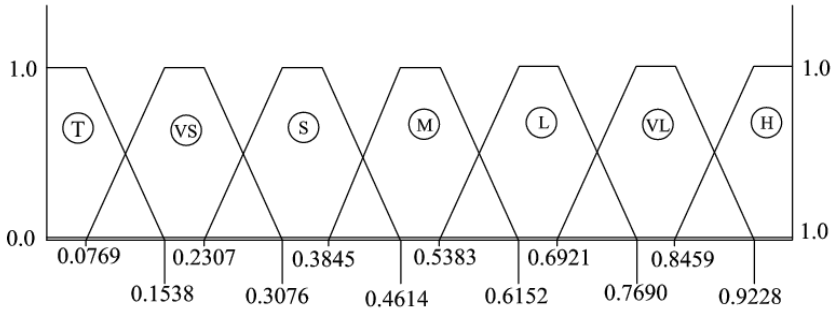

Fig 9: Optimization of Fuzzy Topsis method

The TOPSIS method for multiple attribute optimization, as introduced, offers a solution designed for fuzzy environments that aligns with human cognition in real-world scenarios. In such contexts, uncertainty is typically represented using fuzzy numbers, particularly triangular and trapezoidal, which are well-suited to various engineering settings[20]. Although triangular fuzzy numbers were extensively studied, trapezoidal fuzzy numbers are frequently favored due to their computational simplicity. Represented as (a, b, c, d), trapezoidal fuzzy numbers are considered fundamental because they have a linear membership function, in contrast to triangular fuzzy numbers. This makes them useful for modeling linear uncertainty in numerous engineering applications. In a fuzzy context, linguistic variables are often represented by trapezoidal fuzzy numbers, as shown in Fig. 9. Fuzzy weight numbers, as listed in Table 4, are expressed in linguistic terms. Sivapirakasam[21] elucidates the calculation process, which is similar to that of triangular fuzzy numbers. Table 5. presents the responses of five decision makers, each attribute weight in linguistic terms. The table also displays the average fuzzy weight for each response parameter, derived from the decision maker's inputs.

Table 4. The Linguistic variables for the impotent weight of each output

Fuzzy subsets	Respected fuzzy Weights
Tiny (T)	(0.000, 0.000, 0.077, 0.154)
Very Small (VS)	(0.077, 0.154, 0.231, 0.308)
Small (S)	(0.231, 0.308, 0.385, 0.461)
Medium (M)	(0.385, 0.461, 0.538, 0.615)
Large (L)	(0.538, 0.615, 0.692, 0.769)

Very Large (VL)	(0.692, 0.769, 0.846, 0.923)
Huge (H)	(0.846, 0.923, 1.000, 1.000)

Table 5. Responses for Decision Makers utilizing Fuzzy weights

Responses	Decision Makers (DM)					Fuzzy weights
	DM-1	DM-2	DM-3	DM-4	DM-5	
Hardness	L	VL	H	L	VL	0.661, 0.738, 0.815, 0.877
Tensile Stress	VL	VL	L	VL	H	0.692, 0.769, 0.846, 0.907

Table 6 presents the experimental design matrix along with the normalized response (R_{ij}). The normalized value R_{ij} is calculated using equation 2.

$$R_{ij} = \frac{x_{ij}}{\sqrt{\sum_{i=1}^{12} x_{ij}^2}} \qquad (2)$$

Here, the experimental value x_{ij} corresponds to the i^{th} attribute of the j^{th} experimental run.

Table 6. Value for Normalized matrix (R_{ij})

Sr. No.	R_{ij} of Hardness	R_{ij} of Tensile Stress
1	0.248	0.264
2	0.297	0.306
3	0.283	0.273
4	0.316	0.293
5	0.317	0.300
6	0.296	0.313
7	0.276	0.226
8	0.284	0.298
9	0.280	0.263
10	0.287	0.300
11	0.286	0.311
12	0.289	0.305

In the following step, the factors of the normalized matrix (denoted as R_{ij}) are multiplied by their corresponding fuzzy weights. This produces a weighted performance matrix, represented as S_{ij}, where *i* corresponds to the i^{th} experimental run and *j* corresponds to the j^{th} response, as shown in Table 7. This approach is widely used by researchers[22]. The positive ideal solution (S^+) and the negative ideal solution (S^-) are then defined using the equations (3) and (4), which are presented in Table 8.

$$S^+ = [\max(S_{ij})]\, j\in J \text{ or } [\min(S_{ij})\, j\in J'],\ j=1,2,\ldots\ldots\ 12\ ,\ i=1,.2\ldots..,4 \qquad (3)$$

$$S^- = [\min(S_{ij})]\, j\in J \text{ or } [\max(S_{ij})\, j\in J'],\ j=1,2,\ldots\ldots\ 12 \qquad (4)$$

Here, J pertains to the higher-the-better performance characteristics, while J' pertains to the lower-the-better performance characteristics. In this particular instance, since

all the responses are of the higher-the-better type, only *J* is considered. The attributes of S_{ij} are normalized positive trapezoidal fuzzy numbers, ranging from zero to one[22]. These operations aid in assessing the performance of various experimental runs according to the specified criteria.

Table 7. Weighted normalized matrix of Hv and TS

Run No.	Sij	
	Hv	TS
1	(0.1641, 0.1832, 0.2023, 0.2175)	(0.1825, 0.2027, 0.2230, 0.2392)
2	(0.1965, 0.2194, 0.2422, 0.2605)	(0.2115, 0.2349, 0.2584, 0.2772)
3	(0.1870, 0.2087, 0.2305, 0.2479)	(0.1891, 0.2101, 0.2312, 0.2480)
4	(0.2089, 0.2332, 0.2575, 0.2770)	(0.2029, 0.2255, 0.2480, 0.2661)
5	(0.2099, 0.2343, 0.2587, 0.2782)	(0.2079, 0.2310, 0.2541, 0.2726)
6	(0.1956, 0.2183, 0.2411, 0.2593)	(0.2168, 0.2409, 0.2650, 0.2843)
7	(0.1822, 0.2034, 0.2246, 0.2416)	(0.1564, 0.1737, 0.1911, 0.2050)
8	(0.1880, 0.2098, 0.2317, 0.2491)	(0.2060, 0.2289, 0.2518, 0.2701)
9	(0.1851, 0.2066, 0.2281, 0.2453)	(0.1817, 0.2019, 0.2221, 0.2383)
10	(0.1899, 0.2119, 0.2340, 0.2517)	(0.2074, 0.2304, 0.2535, 0.2719)
11	(0.1889, 0.2108, 0.2328, 0.2504)	(0.2150, 0.2389, 0.2627, 0.2818)
12	(0.1908, 0.2130, 0.2352, 0.2529)	(0.2113, 0.2348, 0.2583, 0.2771)

After calculating this S_{ij} matrix, the next step is to find the distance of positive and negative ideal solutions by using the following equation 5 and 6.

$$d_i^+ = \sum_{i=1}^{12} d(S_{ij}, S_j^+), \quad i=1,2,.....12 \qquad (5)$$

$$d_i^- = \sum_{i=1}^{12} d(S_{ij}, S_j^-), \quad i=1,2,.....12 \qquad (6)$$

$$d(x,y) = \sqrt{\frac{1}{4}[(x_1-y_1)^2+.....+(x_4-y_4)^2]} \qquad (7)$$

Where d(x,y) is the distance between two fuzzy numbers. This distance of two trapezoidal number.

Table 8. Ideal Negative and Ideal Positive values

S_j- and S_j+		
Hv	S_1^-	(0.1641, 0.1832, 0.2023, 0.2175)
	S_1^+	(0.2099, 0.2343, 0.2587, 0.2782)
TS	S_2^-	(0.1564, 0.1737, 0.1911, 0.2050)
	S_2^+	(0.2168, 0.2409, 0.2650, 0.2843)

The fuzzy number is determined using Equation 7, with the values of d^+ and d^- listed in Table 9. Once the distances to the negative and positive ideal solutions are computed, now lastly the closeness coefficient (CC_i) is to be calculated[21]. This coefficient, calculated

with Equation 8, indicates how close ideal solution is to each experimental value. The results are displayed in the same table and illustrated in Figure 10.

$$CC_i = \frac{d_i^-}{d_i^+ + d_i^-} \quad (8)$$

Table 9. Closeness Coefficients (CCi)

Run No.	di-	di+	CCI
1	0.0939	0.0305	0.2449
2	0.0220	0.1024	0.8234
3	0.0592	0.0651	0.5238
4	0.0173	0.1070	0.8605
5	0.0104	0.1140	0.9166
6	0.0168	0.1076	0.8648
7	0.1031	0.0213	0.1712
8	0.0384	0.0860	0.6914
9	0.0701	0.0543	0.4364
10	0.0346	0.0898	0.7220
11	0.0268	0.0975	0.7843
12	0.0288	0.0956	0.7683

5. RESULTS & DISCUSSION

Fig 10: Graph between closeness coefficients with Run number

Following results are observed here:

The comparative examination between 3D printed ABS tensile tests conducted via a Universal Testing Machine (UTM) and enhanced through fuzzy TOPSIS has yielded significant insights into the material's mechanical characteristics. Through UTM tests, empirical data has been garnered, shedding light on the material's practical response to axial forces. Critical mechanical attributes like ultimate tensile strength, yield strength, and elongation at break have been precisely quantified, establishing clear benchmarks for material performance. Noteworthy observations during the UTM test, including deformation patterns and failure modes, contribute to a holistic comprehension of ABS behavior under stress.

A thorough numerical analysis of 12 iteration of this analysis of workpieces employing the fuzzy TOPSIS method has generated specific outcomes. From observations and optimization by fuzzy TOPSIS obtain the value of closeness coefficient CCi is 0.9166 in the fifth run. In the fifth iteration of this analysis, lengths L1 and L2 were determined as 211.56 mm and 198.40 mm, average length is 204.98 respectively, accompanied by a hardness value of 22.0 Hv. Based on these parameters, the optimal configuration ascertained through the fuzzy TOPSIS method was identified at 40.23 MPa. This investigation underscores the potential of the fuzzy TOPSIS-based approach in optimizing the elastic behavior of ABS plastic.

6. CONCLUSION & SCOPE OF FUTURE WORK

This work focuses on analyzing the elastic behavior of ABS plastic by examining its tensile strength, hardness, and surface morphology. The study also introduces a fuzzy TOPSIS-based approach for optimization and multi-criteria decision-making.

TOPSIS (Technique for Order of Preference by Similarity to Ideal Solution) is a multi-criteria decision-making method used to evaluate and rank alternative solutions. In the context of analyzing and optimizing the elastic behavior of ABS plastic, TOPSIS can be applied to select the most suitable combination of parameters or conditions that maximize desired properties such as elasticity, tensile strength and hardness. TOPSIS helps identify the combination of parameters or conditions that yield the most desirable elastic behavior in ABS plastic. TOPSIS also highlights any trade-offs that may exist between different parameters. For example, increasing elasticity might come at the expense of other mechanical properties or processing costs. Understanding these trade-offs is crucial for making well-balanced decisions. Based on these parameters, the optimal setting determined by the fuzzy TOPSIS method was found to be 40.23 MPa. This study demonstrates that the fuzzy TOPSIS-based approach is a promising method for optimizing the elastic behavior of ABS plastic.

From observation with analytical & experimental we can use different setting parameter & condition analytically before actual preparation of sample as the results obtained in both cases are similar in pattern and closer results.

Scope of Future Work:

1. Fatigue Testing
2. Wear Test
3. Torsion Test
4. Bending Test
5. Micro Structure Behaviour using SEM

REFERENCES

[1] S. T. Dwiyati, A. Kholil, R. Riyadi, and S. E. Putra, “Influence of layer thickness and 3D printing direction on tensile properties of ABS material,” in *Journal of Physics: Conference Series*, IOP Publishing Ltd, Dec. 2019. doi: 10.1088/1742-6596/1402/6/066014.

[2] Z. Weng, J. Wang, T. Senthil, and L. Wu, “Mechanical and thermal properties of ABS/montmorillonite nanocomposites for fused deposition modeling 3D printing,” *Mater Des*, vol. 102, pp. 276–283, Jul. 2016, doi: 10.1016/J.MATDES.2016.04.045.

[3] Z. Golubović *et al.*, “A Comprehensive Mechanical Examination of ABS and ABS-like Polymers Additively Manufactured by Material Extrusion and Vat Photopolymerization Processes,”

Polymers (Basel), vol. 15, no. 21, Nov. 2023, doi: 10.3390/polym15214197.

[4] M. Dawoud, I. Taha, and S. J. Ebeid, "Mechanical behaviour of ABS: An experimental study using FDM and injection moulding techniques," *J Manuf Process*, vol. 21, pp. 39–45, Jan. 2016, doi: 10.1016/J.JMAPRO.2015.11.002.

[5] P. Żur, A. Kołodziej, A. Baier, and G. Kokot, "Optimization of Abs 3D-Printing Method and Parameters," *European Journal of Engineering Science and Technology*, 2020.

[6] S. NĂdĂban, S. Dzitac, and I. Dzitac, "Fuzzy TOPSIS: A General View," in *Procedia Computer Science*, Elsevier B.V., 2016, pp. 823–831. doi: 10.1016/j.procs.2016.07.088.

[7] N. Ezhilarasan and C. Vijayalakshmi, "Optimization of Fuzzy programming with TOPSIS Algorithm," in *Procedia Computer Science*, Elsevier B.V., 2020, pp. 473–479. doi: 10.1016/j.procs.2020.05.144.

[8] K. Mirasadi, D. Rahmatabadi, I. Ghasemi, M. Khodaei, M. Baniassadi, and M. Baghani, "Investigating the Effect of ABS on the Mechanical Properties, Morphology, Printability, and 4D Printing of PETG-ABS Blends," *Macromol Mater Eng*, 2024, doi: 10.1002/mame.202400038.

[9] A. Yankin *et al.*, "Optimization of Fatigue Performance of FDM ABS and Nylon Printed Parts," *Micromachines (Basel)*, vol. 14, no. 2, Feb. 2023, doi: 10.3390/mi14020304.

[10] M. Daly, M. Tarfaoui, M. Chihi, and C. Bouraoui, "FDM technology and the effect of printing parameters on the tensile strength of ABS parts," *International Journal of Advanced Manufacturing Technology*, vol. 126, no. 11–12, 2023, doi: 10.1007/s00170-023-11486-y.

[11] A. Farazin and M. Mohammadimehr, "Effect of different parameters on the tensile properties of printed Polylactic acid samples by FDM: Experimental design tested with MDs simulation," *The International Journal of Advanced Manufacturing Technology*, 2021, doi: 10.21203/rs.3.rs-273321/v1.

[12] S. Anand Kumar and Y. Shivraj Narayan, "Tensile testing and evaluation of 3D-printed PLA specimens as per ASTM D638 type IV standard," in *Lecture Notes in Mechanical Engineering*, Pleiades journals, 2019, pp. 79–95. doi: 10.1007/978-981-13-2718-6_9.

[13] C. Horst, S. Tetsuya, and S. Leslie, *Springer handbook of materials measurement methods*, vol. 9, no. 7–8. 2006. doi: 10.1016/s1369-7021(06)71582-6.

[14] P. P. R. Filho, T. Da Silveira Cavalcante, V. H. C. De Albuquerque, and J. M. R. S. Tavares, "Brinell and Vickers hardness measurement using image processing and analysis techniques," *J Test Eval*, vol. 38, no. 1, Jan. 2010, doi: 10.1520/JTE102220.

[15] R. M. R, V. R, and R. S, "Experimental analysis on density, micro-hardness, surface roughness and processing time of Acrylonitrile Butadiene Styrene (ABS) through Fused Deposition Modeling (FDM) using Box Behnken Design (BBD)," *Mater Today Commun*, vol. 27, Jun. 2021, doi: 10.1016/j.mtcomm.2021.102353.

[16] H. Jiang, Q. Gong, M. Peterlechner, L. Daum, H. Rösner, and G. Wilde, "Hardness and microstructural evolution of CoCrFeNi high-entropy alloys during severe plastic deformation," *Materials Science and Engineering: A*, p. 146758, May 2024, doi: 10.1016/j.msea.2024.146758.

[17] J. Gómez-Monterde, M. Sánchez-Soto, and M. L. Maspoch, "Influence of injection molding parameters on the morphology, mechanical and surface properties of ABS foams," *Advances in Polymer Technology*, vol. 37, no. 8, 2018, doi: 10.1002/adv.21944.

[18] B. Neher, Md. A. Gafur, M. A. Al-Mansur, Md. M. R. Bhuiyan, Md. R. Qadir, and F. Ahmed, "Investigation of the Surface Morphology and Structural

Characterization of Palm Fiber Reinforced Acrylonitrile Butadiene Styrene (PF-ABS) Composites," *Materials Sciences and Applications*, vol. 05, no. 06, 2014, doi: 10.4236/msa.2014.56043.

[19] S. Pawanr, T. Tanishk, A. Gulati, G. K. Garg, and S. Routroy, "Fuzzy-TOPSIS based Multi-objective Optimization of Machining Parameters for Improving Energy Consumption and Productivity," in *Procedia CIRP*, Elsevier B.V., 2021, pp. 192–197. doi: 10.1016/j.procir.2021.09.033.

[20] F. Uysal and Ö. Tosun, "Fuzzy TOPSIS-based computerized maintenance management system selection," *Journal of Manufacturing Technology Management*, vol. 23, no. 2. pp. 212–228, 2012. doi: 10.1108/17410381211202205.

[21] S. Rouhani, M. Ghazanfari, and M. Jafari, "Evaluation model of business intelligence for enterprise systems using fuzzy TOPSIS," *Expert Syst Appl*, vol. 39, no. 3, pp. 3764–3771, Feb. 2012, doi: 10.1016/J.ESWA.2011.09.074.

[22] L. Dymova, P. Sevastjanov, and A. Tikhonenko, "An approach to generalization of fuzzy TOPSIS method," *Inf Sci (N Y)*, vol. 238, pp. 149–162, Jul. 2013, doi: 10.1016/j.ins.2013.02.049.